RESEARCH ARTICLE OPEN ACCESS

Computer Aided Kinematic Synthesis Anddynamic Analysis Of Robot End Gripper Mechanism

Sachin Badadhe[1], A P Singh[2], Shantanu Roy[2] and Mukesh Tiwari[2]
[1]*M.Tech. Scholar(Mechanical Engg.) Iist College Indore M.P*
[2] *Professor, Iist College Indore M.P*
Corresponding Author ; Sachin Badadhe

ABSTRACT
In this paper, the new type of Impactive gripper is presented as end effector of robotic gripper. The systematic approach for design of such type robotic gripper is discuss that includes kinematic Synthesis, Static Analysis, and Dynamic Analysis. Respectively the results validationwasperform by graphical method, analytical computation and FEA. The software used for solid modelling – SOLIDWORKS, Mechanism simulation – MSC ADAMS and FEA – ANSYS. The sensitivity analysis of robotic gripper mechanism with variation in link length to achieved the different form configuration and requirements. In dynamic analysis the effect of different magnitude and nature of force and its impact on mechanism behavior is summarize.In transient analysis, the loads fluctuate with time instance and the results of von-mises stresses and deformation for different reach of robotic gripper mechanism.
Keywords-Robotic gripper, Mechanism Synthesis, FEA, Sensitivity Analysis, End effector

---

Date Of Submission:08-10-2018 Date Of Acceptance: 20-10-2018

I. INTRODUCTION

Applications of end gripper is to perform repetitive work processes which are laboriously tiring but rather important usage of end gripper is to access area which are fragile and can be extremely hazardous. Few examples of end grippers, which are use in hazardous area, are

- Handling of Hot metal in steel plants
- Collection of magma samples
- Remote handling and maintenance of objects involving nuclear radiation
- Eradicating mines
- Handling explosive materials
- Decommissioning nuclear facility
- Rescuing people from burning buildings
- Carrying trapped people from collapsed mines
- Disposal of unexploded ordnance,
- Maintenance of steel Bridge structures
- Handling dangerous biological materials and under water engineering work.

Apart from working hazardous areas there is one more application space research that also demands remotely performing space lab activities instead of cost of astronauts labor. Robotic arms fitted with appropriate end-effectors can standby human intrusion in many actions, working independently or being control from less costly earth grounded staff. Purposely designed facilities.

The space research experiments can comprise the manipulation of stuffs of dissimilar nature, not only by shape and size but also from biological aspects. The appropriate gripper mechanisms shall be develop to very specific matters, including the ability of form adaptation with adequate control of gripping forces (delicate handling).

The end grippers are design with parallel moving jaws, which actually meets object. The shape of jaws can be design to suit the form factor of object to be handle and the distance between jaws can vary in wide range according to the width of objects.

In 1969 at Stanford University, an engineer, Victor Scheinman built the Stanford Arm, a robot that was developedentirely for computer control.He built the entire robotic arm on campus, primarily using the shop facilities in the Chemistry Department. The kinematic configuration of the arm included six degrees of freedom with one prismatic and five revolute joints, with brakes on all joints to hold position while the computer calculates the next locationto reach for performing some operation.

In New Jersey, General Motors developedUnimate robots to assemble the Chevrolet Vega automobile parts. At same juncture, manufacturers in japan were making significantrise in manufacturing: reducing costs, standardization, and enhancing efficiency.

Cincinnati Milacron presented a heavy-duty industrial robot called the Cincinnati Milacron T3 (The Tomorrow Tool) robot. Later, Unimation

Incorporated introduced a new series of robots called the PUMA robots.

After the Sept. 11 attacks on twin towers, the collapsed buildings and landscape were too enclosed and dangerous for humans or dogs to navigate. Remote-controlled, small size robots, manufactured by iRobot, these type of robots were the first time reaction to a catastrophe. Because of smaller size, these robots went in narrow spaces to find survivors trapped below building rubble.

In Year 2015, the highest volume robots manufactured recorded.In this year Robot sales increased by 15%.

II. DESIGN OF THE ROBOT GRIPPER

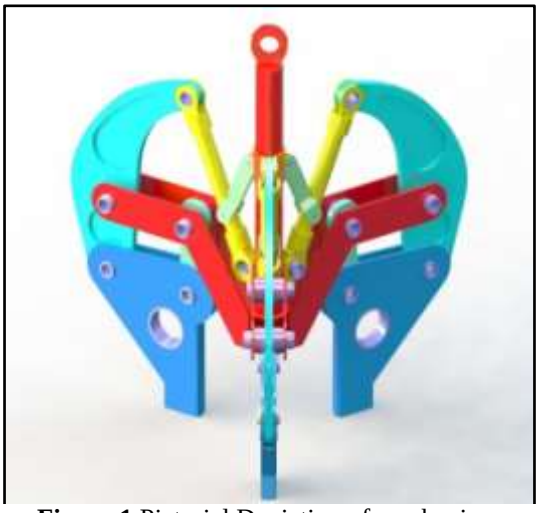

Figure 1 Pictorial Depiction of mechanism

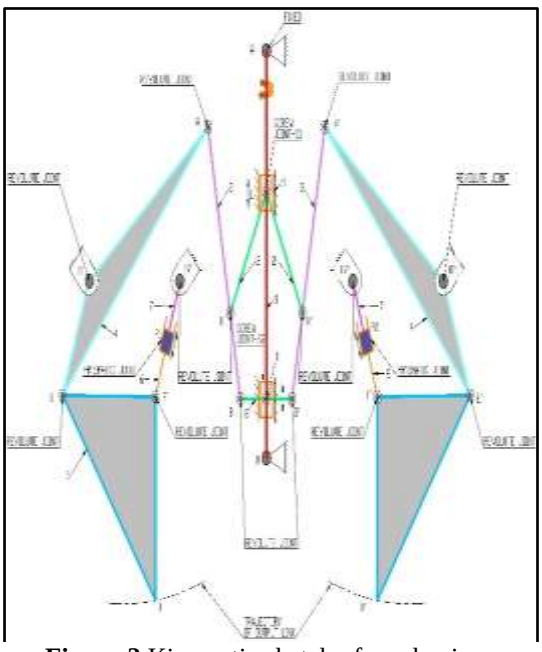

Figure 2 Kinematic sketch of mechanism

Table 1 Inter-Link Joint Details

Jt. No	Joint type	Link-1	Link-2
1	Revolute	Thumb	Ground
2	Revolute	Arm	Ground
3	Revolute	Arm	Tong
4	Revolute	Thumb	Tong
5	Revolute	Arm	Shoulder
6	Revolute	Shoulder	Main rod
7	Revolute	Conn. Link	Shoulder
8	Revolute	Conn. Link	Pin
9	Revolute	Main rod	Pin
10	Revolute	Thumb	Ground
11	Revolute	Arm	Ground
12	Revolute	Arm	Tong
13	Revolute	Thumb	Tong
14	Revolute	Shoulder	Arm
15	Revolute	Shoulder	Main rod
16	Screw	Sleeve 1	Main rod
17	Revolute	Conn. Link	Shoulder
18	Revolute	Main rod	Ground
19	Screw	Sleeve 2	Main rod
20	Prismatic	Thumb	Ground
21	Prismatic	Thumb	Ground

This mechanism is blend two very common mechanisms, lower half is four bar mechanism with one flexible link and upper half is Inversion of slider crank mechanism (Refer fig 3). In four bar mechanism there two cranks one is Arm (Part 5) whose other end is driven by movement of shoulder(Part 2), connecting links (part 3), sleeves (part 8 and 9) and Main rod (Part 1). The other crank in four bar mechanism is flexible

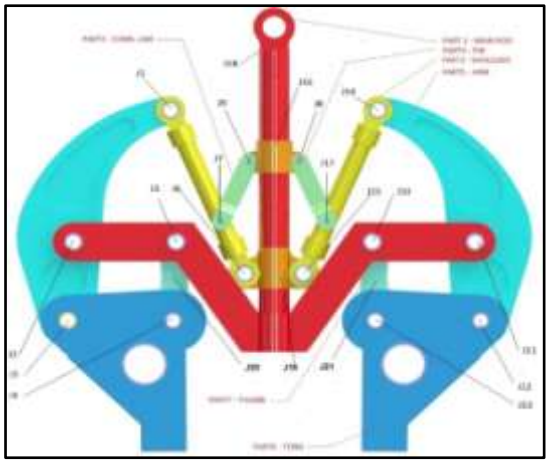

Figure 3 Mechanism with joint details

length of the Thumb link (part 7) which rotates to accommodate the change in length.

In this mechanism, the Arm (part 5) and Thumb (part 7) are attach to structure which as grounded. Upper half of Arm (Part 5) is connected to Shoulder (Part 2) with revolute joint. Shoulder (part 2) is attached to Sleeve (Part 8 and 9) at two locations, one with direct connection and another with connecting link (Part 3) with revolute joint. Main rod has Y-Axis Prismatic Joint with Ground as it rotates on bearings. Whole arrangement is symmetrical about vertical axis of Main rod (Part 1). All the revolute joints are fix on pins.

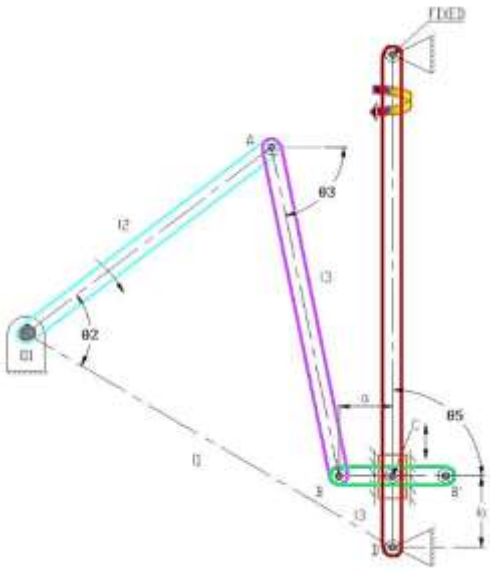

Figure 4 Synthesis of Mechanism -1

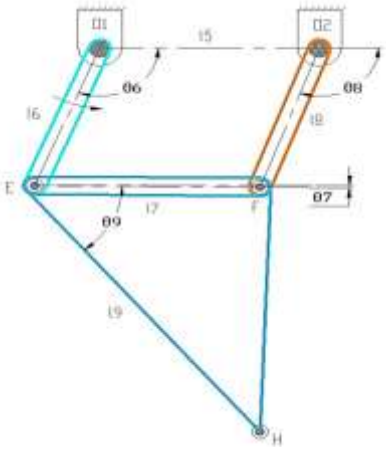

Figure 5 Synthesis of Mechanism -2

We start the analysis by defining vectors and constructing the vector loop equation: For Mechanism-1

$$R_{AO_2} + R_{BA} + R_{CB} + R_{DC} - R_{DO_2} = 0 \quad (1)$$

The constant lengths are: $R_{AO_2} = l_2,\ R_{BA} = l_3\ , R_{CB} = a,\ R_{DC} = l_4,\ R_{DO_2} = l_1$

We define an angle (orientation) for each vector according to our convention (CCW with respect to the positive x-axis).

Position equations

The vector loop equation is projected onto the x and y axes to obtain two algebraic equations

$$R_{AO_2}\cos\theta_2 + R_{BA}\cos\theta_3 + R_{CB}\cos\theta_4 + R_{DC}\cos\theta_5 - R_{DO_2}\cos\theta_1 = 0 \quad (22)$$

$$R_{AO_2}\sin\theta_2 + R_{BA}\sin\theta_3 + R_{CB}\sin\theta_4 + R_{DC}\sin\theta_5 - R_{DO_2}\sin\theta_1 = 0 \quad (3)$$

Now since $\theta_1 = 0°,\ \theta_4 = 0°,\ \theta_5 = 90°$,
We have:

$$l_2\cos\theta_2 + l_3\cos\theta_3 + a - l_1 = 0 \quad (4)$$
$$l_2\sin\theta_2 + l_3\sin\theta_3 + l_4 = 0 \quad (5)$$

These equations represented in matrix form,

$$\begin{bmatrix} l_2\cos\theta_2 & l_3\cos\theta_3 \\ l_2\sin\theta_2 & l_3\sin\theta_3 \end{bmatrix} = \begin{bmatrix} l_1 - a \\ l_4 \end{bmatrix}$$

Velocity Equations

The time derivative of the position equations yields the velocity equations: for Mechanism-1

$$-l_2\sin\theta_2\omega_2 - l_3\sin\theta_3\omega_3 = 0 \quad (6)$$
$$l_2\cos\theta_2\,\omega_2 + l_3\cos\theta_3\,\omega_3 + l_1' = 0 \quad (7)$$

These equations represented in matrix form, where the terms associated with the known Slider velocity shifted to the right-hand-side:

$$\begin{bmatrix} -l_2 \sin\theta_2 & -l_3 \sin\theta_3 \\ l_2\cos\theta_2 & l_3\cos\theta_3 \end{bmatrix}\begin{bmatrix} \omega_2 \\ \omega_3 \end{bmatrix} = \begin{bmatrix} 0 \\ -l_1' \end{bmatrix}$$

Acceleration equations
The time derivative of the velocity equations yields the acceleration equations: for Mechanism-1

$-l_2 \sin\theta_2\omega_2 - l_3 \sin\theta_3\omega_3 = 0$ (8)
$l_2 \cos\theta_2\ \omega_2 + l_3 \cos\theta_3\ \omega_3 + l_1' = 0$ (9)

$-l_2 \sin\theta_2 \propto_2 - l_2 \cos\theta_2\omega_2^2 - l_3 \sin\theta_3 \propto_3 -$
$l3\cos\theta3\omega32 = 0$ (10)

$l_2 \cos\theta_2 \propto_2 - l_2\ sin\ \theta_2\omega_2^2 + l_3\ cos\ \theta_3 \propto_3 -$
$l3 sin\theta3\omega32 + l1: = 0$ (11)

These equations represented in matrix form, where the terms associated with the known slider acceleration and the quadratic velocity terms shifted to the right-hand-side:

$$\begin{bmatrix} -l_2\ sin\theta_2 & -l_3\ sin\theta_3 \\ l_2 cos\theta_2 & l_3 cos\theta_3 \end{bmatrix}\begin{bmatrix} \propto_2 \\ \propto_3 \end{bmatrix} = \begin{bmatrix} l_2\ cos\ \theta_2\ \omega_2^2 + l_3\ cos\ \theta_3\omega_3^2 \\ -l_1 + l_2\ sin\ \theta_2\omega_2^2 + l_3\ sin\ \theta_3\omega_3^2 \end{bmatrix}$$

The vector loop equation for Mechanism-2
$R_{EO_2} + R_{FE} - R_{O_1F} - R_{O_1O_2} = 0$ (12)
$R_{EO} = l_6, \quad R_{FE} = l_7, R_{O_1F} = l_8, \ R_{O_1O_2} = l_5$

Position equations
The vector loop equation projected onto the x- and y-axes to obtain two algebraic equations: for Mechanism-1

$R_{EO_2}\cos\theta_6 + R_{FE}\cos\theta_7 - R_{O_1F}\cos\theta_8 -$
$R_{O_1O_2}\cos\theta_5 = 0$ (13)
$R_{EO_2}\sin\theta_6 + R_{FE}\sin\theta_7 - R_{O_1F}\sin\theta_8 -$
$R_{O_1O_2}\sin\theta_5 = 0$ (14)

Since, $\theta_5 = 0°$, and the link lengths are known constants, the equations are simplified to
we have:

$l_6\cos\theta_6 + l_7\cos\theta_7 - l_8\cos\theta_8 - l_5 = 0$ (15)
$l_6\sin\theta_6 + l_7\sin\theta_7 - l_8\sin\theta_8 = 0$ (16)

$$\begin{bmatrix} l_6 cos\theta_2 & l_7 cos\theta_3 & -l_8\cos\theta_8 \\ l_2 sin\theta_2 & l_3 sin\theta_3 & -l_8\sin\theta_8 \end{bmatrix} = \begin{bmatrix} l_5 \\ 0 \end{bmatrix}$$

Velocity equations
The time derivative of the position equations yields:

$-l_6\sin\theta_6\omega_6 - l_7\sin\theta_7\omega_7 + l_8\sin\theta_8\omega_8 = 0$
(17)
$l_6\cos\theta_6\omega_6 + l_7\cos\theta_7\omega_7 - l_8\cos\theta_8\omega_8 = 0$ (18)

The angular velocity of the crank, ω_6, known; we re-arrange and express these equations in matrix form as

$$\begin{bmatrix} -l_7\ sin\theta_7 & l_8\ sin\theta_8 \\ l_7 cos\theta_7 & -l_8 cos\theta_8 \end{bmatrix}\begin{bmatrix} \omega_7 \\ \omega_8 \end{bmatrix} = \begin{bmatrix} l_6\ sin\ \theta_6\omega_6 \\ -l_6\ cos\ \theta_6\omega_6 \end{bmatrix}$$

Acceleration equations
The time derivative of the velocity equations yields the acceleration equations: for Mechanism-2

$-l_6\ sin\ \theta_6 \propto_6 - l_6\ cos\ \theta_6\omega_6^2 -$
$l_7\ sin\ \theta_7 \propto_7 - l_7\ cos\ \theta_7\omega_7^2 + l_8\ sin\ \theta_8 \propto_8 +$
$l_8\ cos\ \theta_8\omega_8^2 = 0$ (19)

$l_6\ cos\ \theta_6 \propto_6 - l_6\ sin\ \theta_6\ \omega_6^2 + l_7\ cos\ \theta_7 \propto_7 -$
$l_7\ sin\ \theta_7\omega_7^2 - l_8\ cos\ \theta_8 \propto_8 + l_8\ sin\ \theta_8\omega_8^2 = 0$
(20)

Now that we know α_6, we re-arrange the equations and rewrite in matrix form

$$\begin{bmatrix} -l_7 s\theta_7 & l_8 s\theta_8 \\ l_7 c\theta_7 & -l_8 c\theta_8 \end{bmatrix}\begin{bmatrix} \propto_7 \\ \propto_8 \end{bmatrix} = \begin{bmatrix} l_6(s\theta_6 \propto_6 + c\theta_6\omega_6^2) + l_7 c\theta_7\omega_7^2 - l_8 c\theta_8\omega_8^2 \\ -l_6(c\theta_6 \propto_6 - s\theta_6\omega_6^2) + l_7 s\theta_7\omega_7^2 - l_8 s\theta_8\omega_8^2 \end{bmatrix}$$

In addition to solving the kinematic equations for the coordinates, velocities and accelerations of lower mechanism, we may need to determine the kinematics of a point of contact on Jaws (link) of the mechanism. Determining the kinematics of a point on the jaw is a secondary process and it does not require solving any set of algebraic equations, we only need to evaluate one or more expressions.
We can consider the point of contact on jaw as Four-bar coupler point

The coupler of a lower four-bar is in the shape of a triangle, and the location of the coupler point H relative to E and F defined by angle θ_9 and length L_9. This coupler positioned with respect to O_2 with x-y frame
Coupler point equations
$X_H = l_6\cos\theta_6 + l_9\cos(\theta_9 + \theta_7)$ (21)
$Y_H = l_6\sin\theta_6 + l_9\sin(\theta_9 + \theta_7)$ (22)
The time derivative of the position expressions provides the velocity of point H:

$X_H^{'} = -l_6 \sin\theta_6\omega_6 - l_9 \sin(\theta_9+\theta_7)\,\omega_7$ (23)
$Y_H^{'} = l_6 \cos\theta_6\omega_6 + l_9 \cos(\theta_9+\theta_7)\,\omega_7$ (24)
Similarly, the time derivative of the velocity expressions yields the acceleration of point H:
$X_H^{''} =$
$-l_6(\sin\theta_6 \propto_6 + \cos\theta_6\omega_6^2) - l_9[\sin(\theta_9+\theta_7) \propto_7 + \cos(\theta_9+\theta_7)]\,\omega_7^2$ (25)
$Y_H^{''} =$
$l_6(\cos\theta_6 \propto_6 - \sin\theta_6\omega_6^2) + l_9[\cos(\theta_9+\theta_7) \propto_7 - \sin(\theta_9+\theta_7)]\,\omega_7^2$ (26)
Velocity Analysis approach using Jacobian
$\frac{dC}{dt} = 0 = \frac{\partial C}{\partial q}\frac{\partial q}{\partial t} + \frac{\partial C}{\partial t}$ (27)
$\frac{\partial C}{\partial q} = [C_q],\ \frac{\partial q}{\partial t} = \{q_i\},\ \frac{\partial C}{\partial t} = [C_t],$ (28)
$[C_q]\{q_i\} + [C_t]$ (29)
$[C_q]\{q_i\} = -[C_t]$ (30)
$\{q_i\} = -[C_q]^{-1}[C_t]$ (31)
Acceleration Analysis approach using Jacobian
$\frac{d}{dt}([C_q]\{q_i\} + [C_t]) = 0$ (32)
$\frac{d}{dt}[[C_q]\{\dot{q}_i\}] + \frac{d}{dt}[C_t]) = 0$ (33)
$\frac{d}{dt}\left[[C_q]\{\dot{q}_i\}\right] = \frac{\partial}{\partial q}\left[[C_q]\{\dot{q}_i\}\right]\{\dot{q}_i\} + \frac{\partial}{\partial t}\left[[C_q]\{\dot{q}_i\}\right]$ (34)
$\left[[C_q]\{\dot{q}_i\}\right]_q \{\dot{q}_i\} + \left[[C_{qt}]\{\dot{q}_i\}\right] + \left[[C_q]\{\ddot{q}_i\}\right]$ (35)
$\frac{d}{dt}[C_t] = \frac{\partial}{\partial q}[C_t]\frac{\partial q}{\partial t} + \frac{\partial}{\partial t}[C_t]$ (36)
$\left[[C_{qt}]\{\dot{q}_i\}\right] + \{C_{tt}\}$ (37)
$\left[[C_q]\{\dot{q}_i\}\right]_q \{\dot{q}_i\} + \left[[C_{qt}]\{\dot{q}_i\}\right] + \left[[C_q]\{\ddot{q}_i\}\right] + \left[[C_{qt}]\{\dot{q}_i\}\right] + \{C_{tt}\} = 0$ (38)
$\left[[C_q]\{\dot{q}_i\}\right]_q \{\dot{q}_i\} = -\left[[C_{qt}]\{\dot{q}_i\}\right] - 2\left[[C_q]\{\ddot{q}_i\}\right] - \{C_{tt}\} = 0$ (39)

In this end gripper mechanism driving motion is initiated through Main Rod (Part 1), which is grounded part. Main Rod is having rotary motion about y-axis. The Motion is generate by combination of gearbox and electric AC motor. The Prime mover can be squirrel cage motors controlled by VVVF drives or servomotor, which can provide accurate position. The Main rod (Part 1) have external threads and assembled with Sleeves (Part 8 and 9) which have internally threads. The downward movement of Sleeves results in Outward travel of Jaws (part 6). In addition to this, there is one more input motion translating which helps jaws (part 6) to attain object form. This motion is achieve by application hydraulic system at prismatic joint. In computer-aided simulation, the motions are in terms of combination of polynomial step functions.

Desired output motion of jaws (part 6) is achieve with kinematics of connecting link (part 3), Shoulder (part 2) and arm (part 5). The displacement of output component is angular which can manipulated based on application of mechanism. Output Motion have three speed variations. In the first phase speed shall be high and then it later phases speed shall reduce as both jaws approach closer. This speed variation is necessary to operator to ensure secure tight grip between jaws and object.

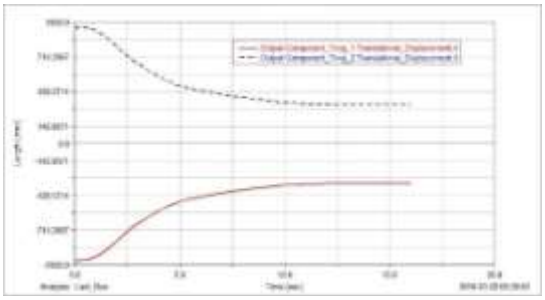

Figure 6 Expected Displacement Profile of Output Component

In above Fig. the expected displacements of robotic gripper jaws shown. This robotic gripper intended to work with minimum total displacement of Jaws of 700 mm. Both the jaws will travel in opposite direction. Therefore expected displacement shows open position of ± 1000 to ± 300 mm. Now to operate the robotic gripper smoothly it is very essential that the mechanism is starting very slowly and during middle of the motion, it reaches to its max velocity and then just before jaws reaches object its starts reducing velocity, which is nothing but the retardation phase.

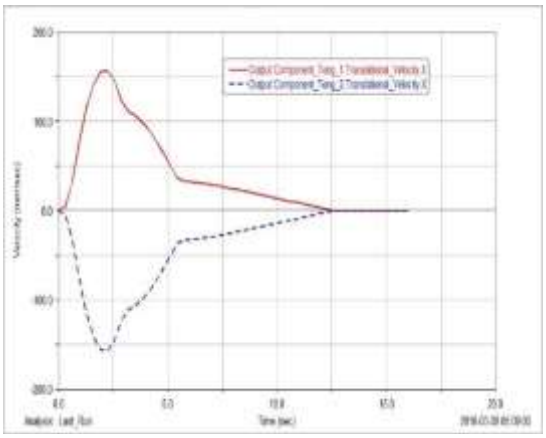

Figure 7 Expected Velocity Profile of Output Component

From above Fig. three phases of robotic gripper mechanism shown. Phase1 is starting phase wherein the mechanism starts from rest position at low velocity of about 5 mm/sec. Then in Phase 2 the robotic gripper has already in motion and velocity changes at constant rate from 50 mm/sec to 200 mm/sec. At the end the robotic gripper, enter into phase III when the retardation starts. In here the robotic gripper jaws are about to reach the object and the velocity reduces in 2 steps from 200 mm/sec

to 50 mm/sec and 50 mm/sec to 0 mm/sec. During this jaws apply enough pressure to hold the object firmly.

III. KINEMATIC SIMULATION

A kinematic model is used to find the resultant output Jaw tip velocities that allow for any type of operator defined motion of the robotic gripper. It is assumed that an operator defines the following parameters when operating the robotic gripper

• Driving Speed.
• Jaw angular velocity and Jaw Position.
• Resultant Force on Jaws.

This kinematic model takes advantage of the robotic gripper's ability to open and close itself. The first step in formulating this model is to develop the forward kinematics of the robotic gripper that gives the motion of the robotic gripper's body coordinate frame corresponding to the global frame as a function of its joints positions and user-defined velocities. The next step is to find the force needed to grip and hold the object firmly without any relative motion. The resultant velocity vector characterizes the arrangement of user-defined motion of opening and closing the robotic gripper.
To frame the forward kinematic relationship between the robotic gripper and its linkages, it is first necessary to assign coordinate frames to each of the joints that connected by the movement of the Jaws.

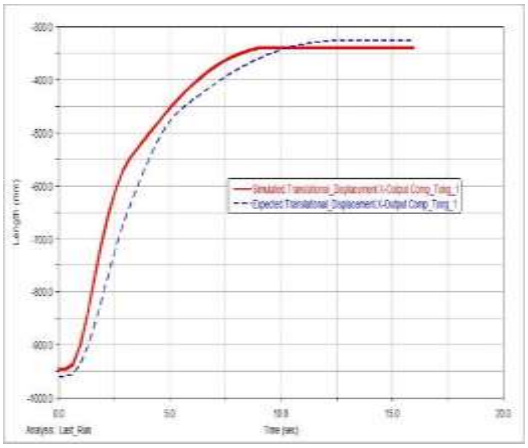

Figure 8 Simulated and Expected Displacement Profile of the Output Jaws

The kinematic simulation been carried out on software MSC Adams 2013. The step function applied to Main rod (input) to get the desired trajectory of output jaws of robotic gripper. By use of step,function still there was continual trajectory difference between expected and simulated displacement. To minimize this difference the inverse kinematics approach can be use.

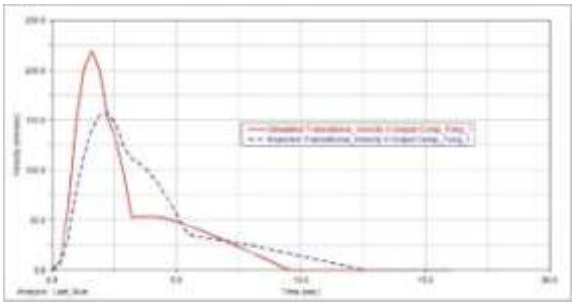

Figure 9 Simulated and Expected Velocity Profile the Output Jaws

Similar difference to the displacement profile carried forward in velocity profile as shown in Fig.9. Author intended to minimize this difference to get the accurate positon of mechanism.

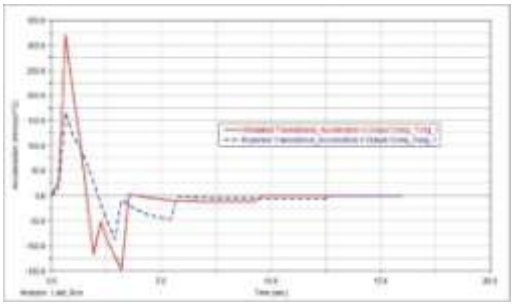

Figure 10 Simulated and Expected Acceleration Profile of the Output Jaws

Overall simulated displacement of output Tongs/jaws is closer to required however, there is considerable difference between simulated and expected velocity and acceleration. The output component travels less with respect to input link Part 1. In my view in such cases, Inverse Kinematics approach shall opted to get values of simulated kinematics parameters closer to expected one. In addition, to minimize the jerk of mechanism the polynomial displacement function need to apply which shall reduce the rate of change of acceleration.

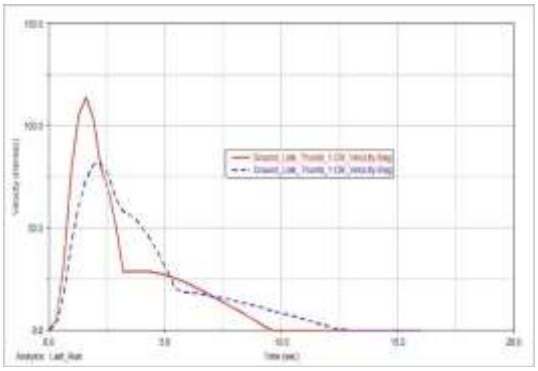

Figure 11 Simulated and expected velocity profile of thumb.

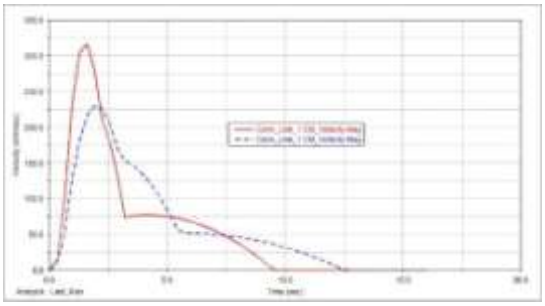

Figure 12 simulated and expected velocity profile of conn. Link.

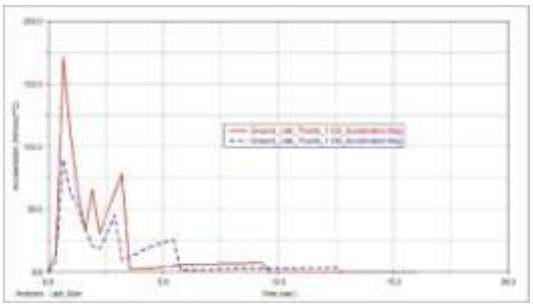

Figure 13 simulated and expected acc. Profiles of thumb.

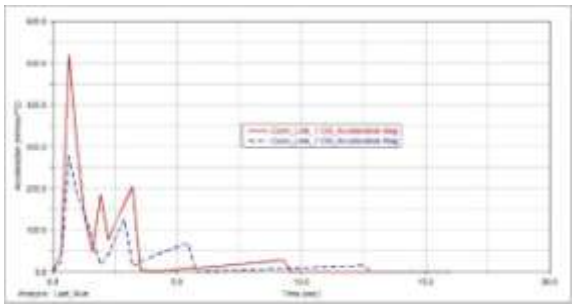

Figure 14 simulated and expected acc. Profiles of conn. Link.

1.1 Sensitivity Analysis

For mechanism sensitivity analysis, we have made 2 changes. The length of Arm (Part 5) is increased by 100 mm whereas on the other hand length of Shoulder (Part 2) is reduced by 100 mm. Below are results plotted. From the plots it appears clearly that the change in length of links affects proportional varies the displacement of gripper jaws however there is nearly no change in velocity and subsequently acceleration plots. The change in link length of 100 mm in both Arm and Shoulder reduces displacement of robotic gripper by 50 mm.

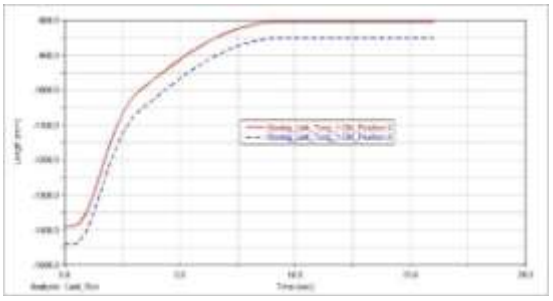

Figure 15 Displacement Sensitivity of the Conn. Link.

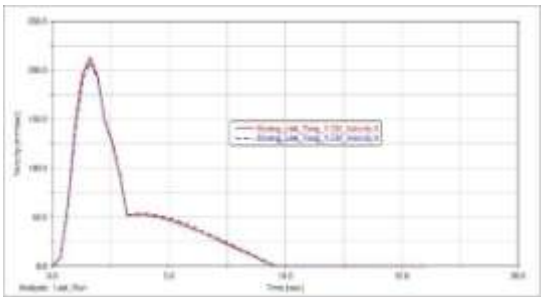

Figure 16 Velocity Sensitivity of the Conn. Link.

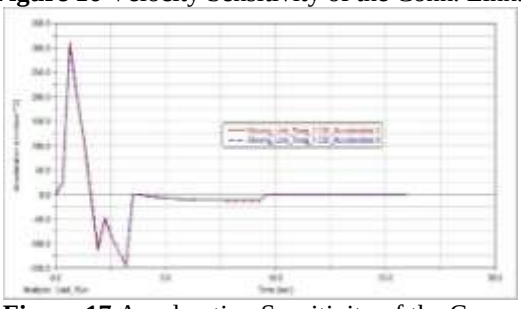

Figure 17 Acceleration Sensitivity of the Conn. Link.

IV. VALIDATION OF KINEMATIC SIMULATION

From Fig. 18 the mechanism modeled in 3D modelling software to do position analysis. The robotic gripper been set at four different position from its initial open position. By graphical method, the displacement of output jaws measure with respect to corresponding movement of input Main Rod. The output displacement found to be very close to the simulated result (Refer Fig. 19).

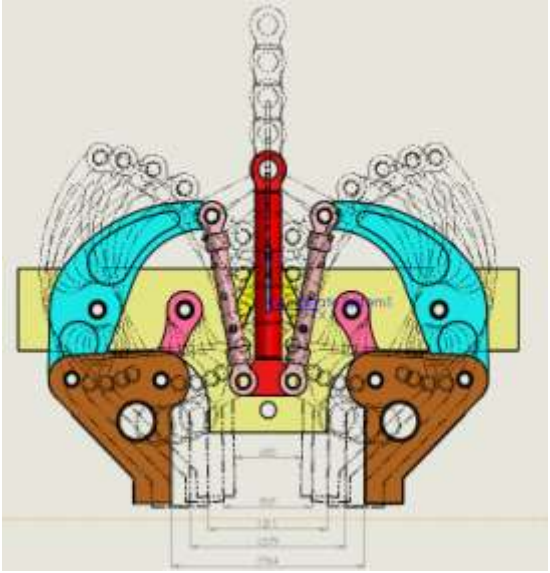

Figure 18 Array of Alternate positions of Mechanism Embossed on one another

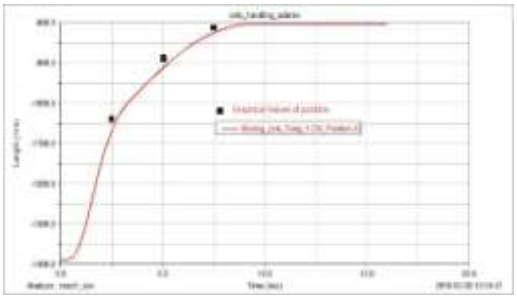

Figure 19 Simulated and Graphical Method Displacement Profiles of Output Component.

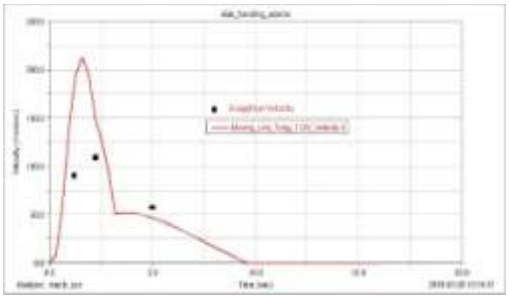

Figure 20 Simulated And Graphical Velocity Profile Of The Output Component.

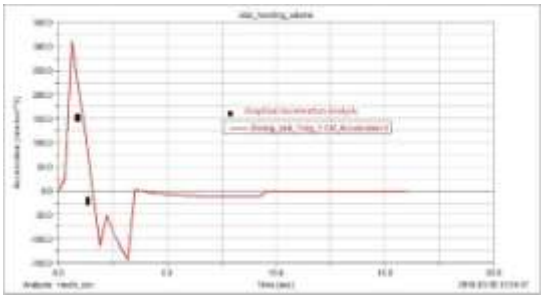

Figure 21 Simulated And Graphical Acceleration Profile Of The Output Component.

V. STATIC ANALYSIS

A constant force in a global direction is applied to the tip of the output component (Jaw Part 6) also the reactive force required at the driving component (Main Rod Part 1) to hold the mechanism stationary at four different position under this condition is obtained using commercial software package MSC ADAMS 2013. The direction of the force applied at the same chosen location in global coordinates. The point and direction of application and magnitude of these forces shown in four different snapshots as below.

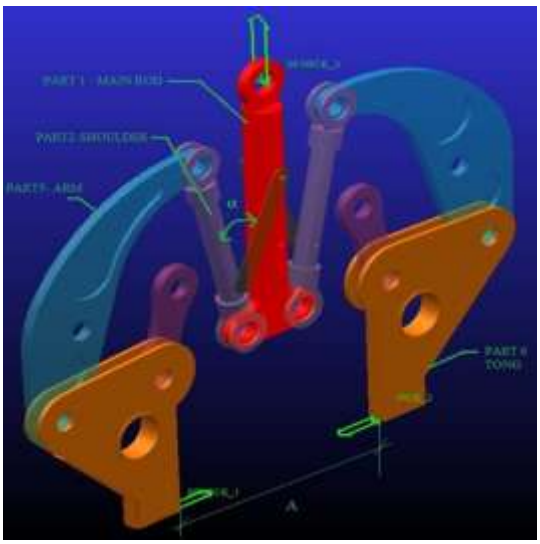

Figure 22 Point and direction of application of forces In above Static force evaluation exercise was prima fascia a trial error approach applied however, this approach was very time consuming and the mechanism never attains equilibrium position. Later on I have use structural Analysis approach wherein driving component givenfixed constraints and the External Forces were implied onto the tip of output Body Refer below Figures).

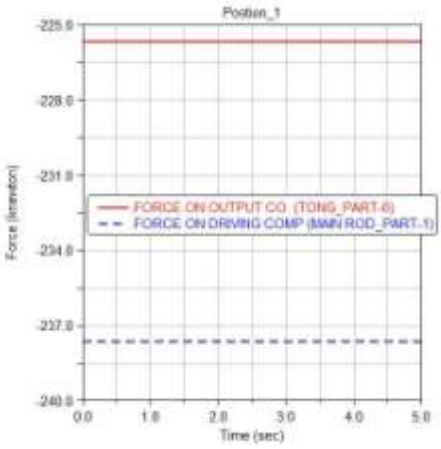

Figure 23 Static Force Analysis In position 1- α – 13.18 ˚ and A = Distance between Jaws– 1890 mm

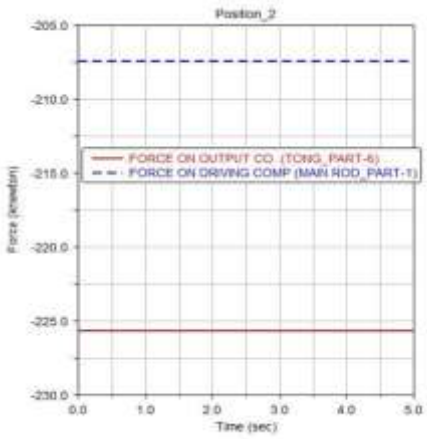

Figure 24 Static Force Analysis In position 2- α – 37.38 ˚ and A = Distance between Jaws– 1125 mm

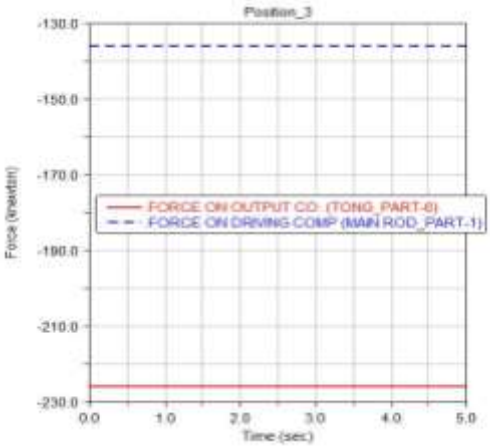

Figure 25 Static Force Analysis In position 3- α – 53.98 ˚ and A = Distance between Jaws– 790 mm

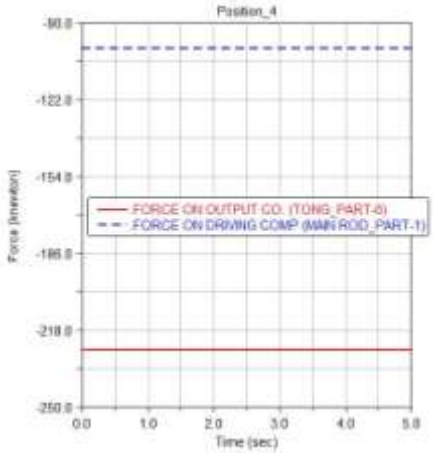

Figure 26 Static Force Analysis In position 4- α – 61.75 ˚ and A = Distance between Jaws– 680 mm

From Above observation the magnitude of driving force increases with increase in distance between tongs (A) and decrease in Angle α. Where α is the angle between shoulder part 2 and Main rod Part 1.

Table 2 Summery of Static Analysis

Position No.	α (Deg)	Dist. Bet. Jaws - m	Effort on I/p Comp. (MSC Adams) - KN	Effort on I/p Comp. (Manual Computation)
1	13.18	1.8	226	220
2	37.38	1.125	207.5	200
3	53.93	0.78	138	145
4	61.75	0.68	103	115

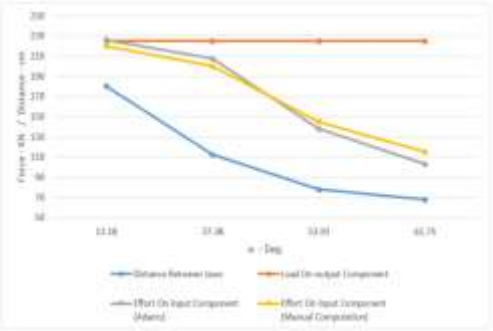

Figure 27 Graphical Representation variation of effort required at different positions of mechanism.

VI. DYNAMIC ANALYSIS

1.2 Constant Driving Force F – 259.45 KN

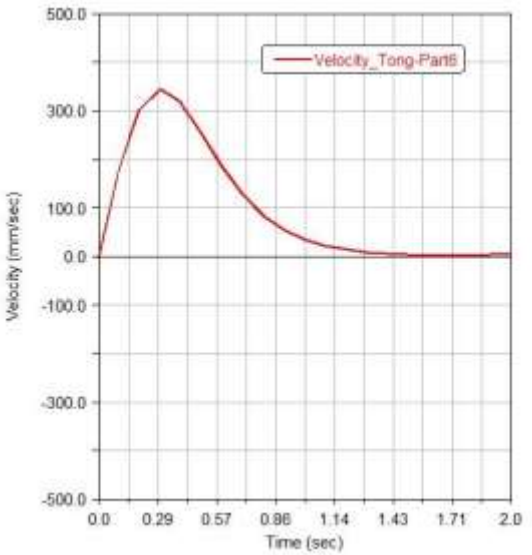

Figure 28 Velocity Plot for Output Component

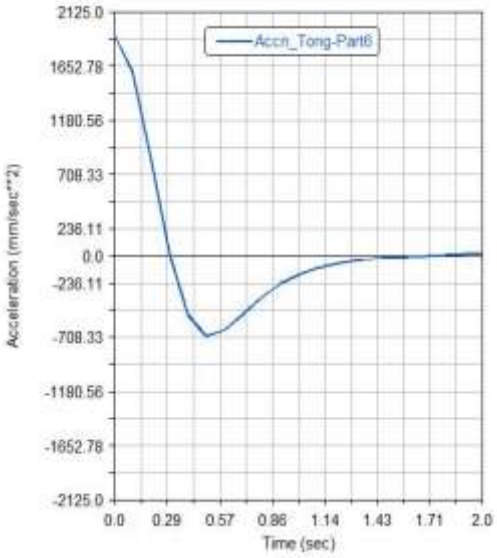

Figure 29 Accn. Plot for Output Component

1.3 Constant Driving Force 2F – 518.90 KN

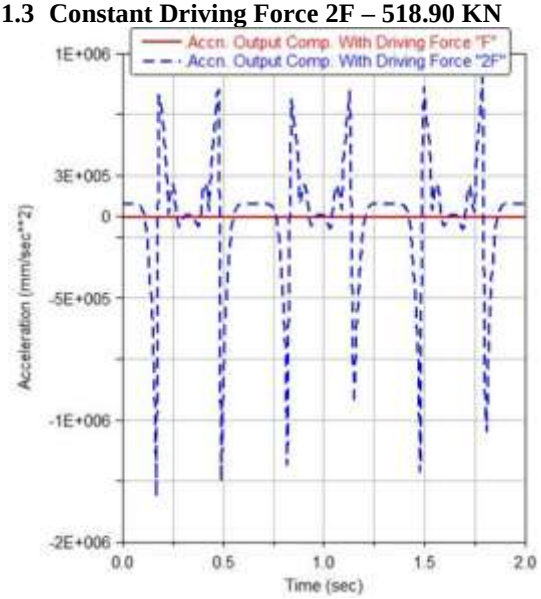

Figure 30 Velocity Plot for Output Component

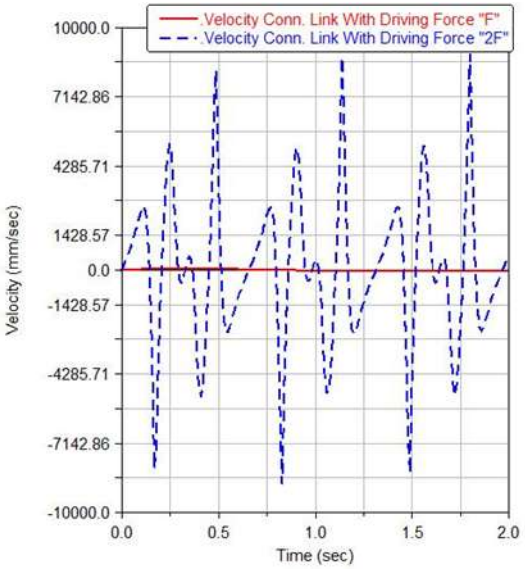

Figure 31 Accn. Plot for Output Component

From above plots, we can see that if we increase the value of force above the certain min magnitude then the mechanism undergoes abrupt periodic motion. This is because of the unbalance in gravitational moment and moment due to external forces. The pattern shows the continual change in velocity and acceleration.

1.4 Sinusoidal Force 1.4F – 362.25 KN

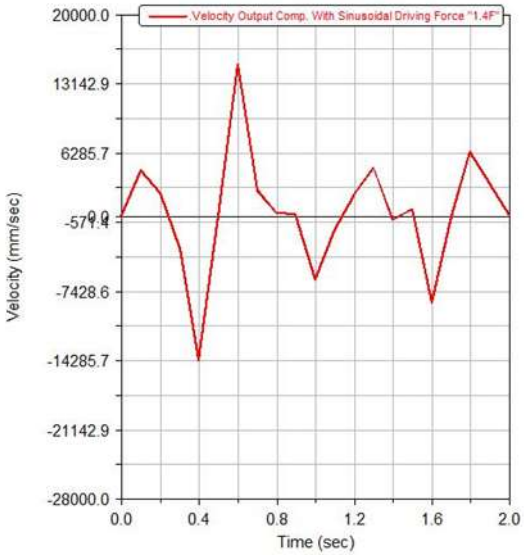

Figure 32 Velocity Plot for Output Component

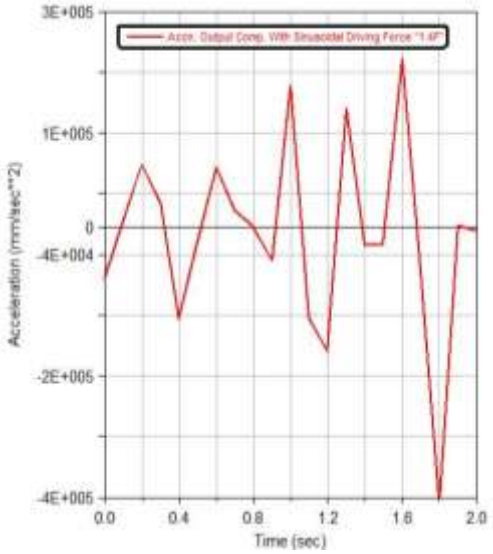

Figure 33 Accn. Plot for Output Component

1.5 Sinusoidal Force 2x1.4F – 726.45 KN

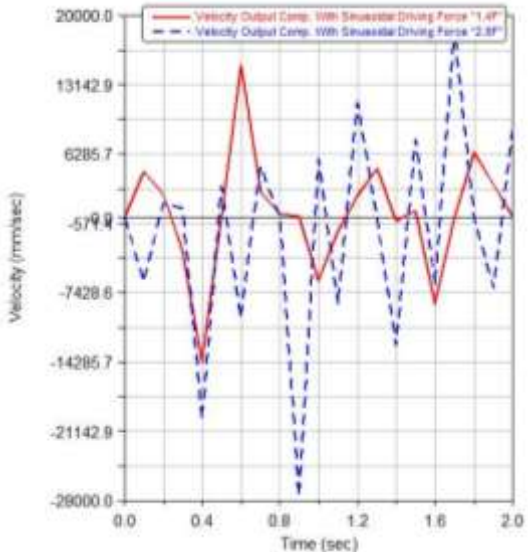

Figure 34 Superimposed Velocity Plot for Output Comp.

From Above plots, we can conclude that if we change the nature of force that is from constant to sinusoidal the mechanism oscillates because of simple harmonic motion. The amplitude of this oscillation depends upon the magnitude if sinusoidal force applied on driving component. In addition, the velocity and acceleration plots are Sinusoidal in nature.

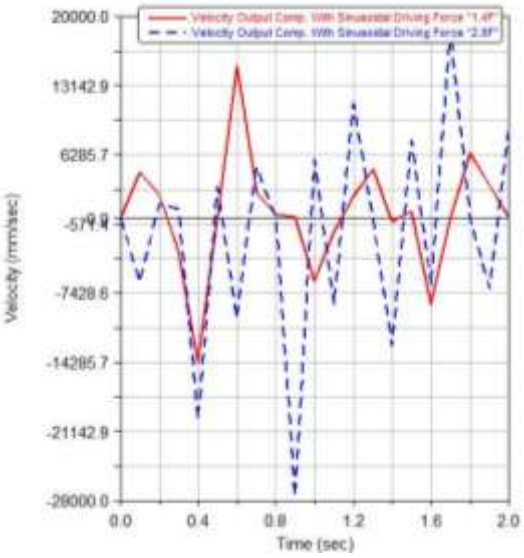

Figure 35 Superimposed Accn. Plot for Output Component

VII. FINITE ELEMENT ANALYSIS

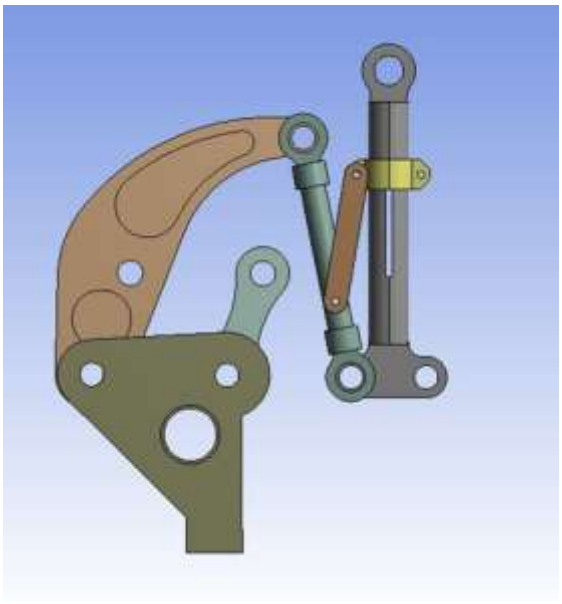

Figure 36 Model View

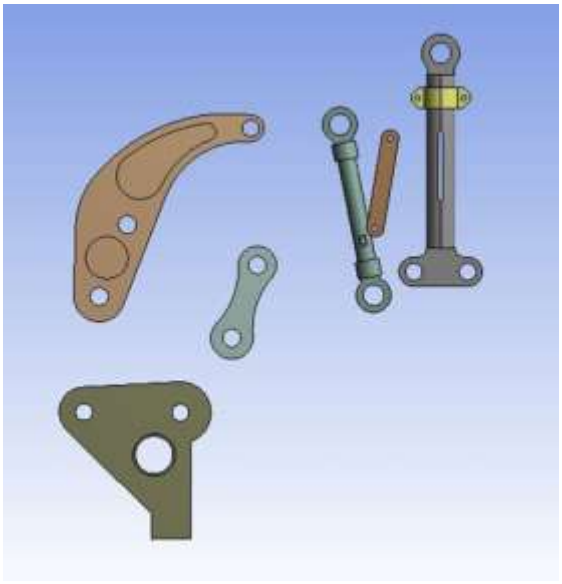

Figure 37 Exploded Model View

Table 3 Material Properties

Object Name	Geometry
Length X	2645.1 mm
Length Y	3437.6 mm
Length Z	326. mm
Volume	2.7739e+008 mm³
Bodies	7
Nodes	130394
Elements	35481

Table 4 Structural Steel - Constants

Density	7.85e-006 kg mm^-3
Comp. Yield Strength	250 MPa
Tensile Yield Strength	250 MPa
Tensile Ult. Strength	460 MPa
Young's Modulus	2.e+005 MPa
Poisson's Ratio	0.3
Shear Modulus	76923 MPa

a. Boundary Conditions

Robotic Gripper Mechanism for carrying out static and Transient analysis different boundary conditions are applied. In static Analysis the output component which jaw is consider to be fix and force of 259.5 KN is applied to input component Main Rod as shown below. In addition, the transient structural analysis results achieved with help of joints in the assembly.

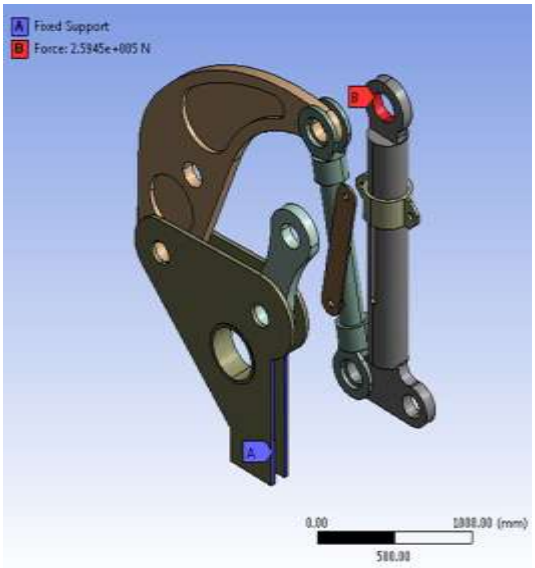

Figure 38 Boundary Conditions –Load 259.45 N.

b. Mesh Modelling

Meshing of the Robotic Gripper model was done after defining the material properties and assigning each material to each of the component. Mesh convergence test first performed for deciding the element size for meshing of the model.

7.2.1 Mesh convergence test

By using mesh convergence test a checkpoint tested on the assembly. This was done in order to simplify and justify the analysis result. In this process the von- misses stress level was tested on assembly by taking different size of element during meshing. With the assistance of ANSYS-16.2 software, the respective mesh sizes with corresponding Total deformation. So mesh refining test are required to check whether the final value are independent are not hence grid independence test were performed to get the result of the Robotic Gripper.Hex dominant elements used for all the components of Robotic Gripper. Hex dominant, which means that the majority of elements are Brick/Hex type and to better approximate the body shape tetrahedral elements used wherever necessary. Meshed Robotic Gripper and details of no. of element and nodes shown below.

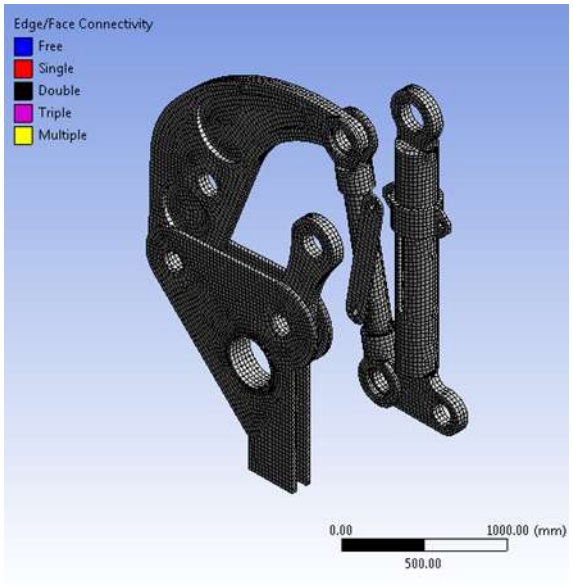

Figure 39 Mesh Plot

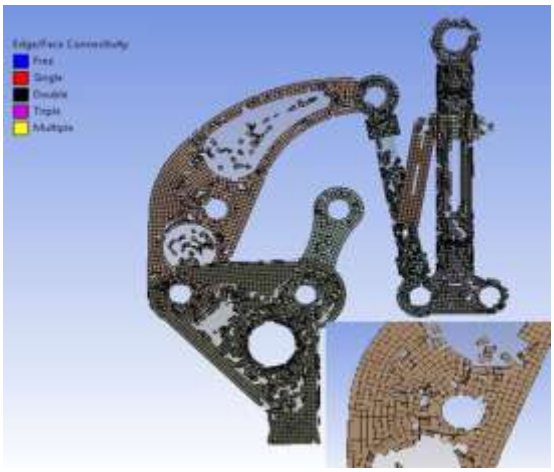

Figure 40 Mesh Quality

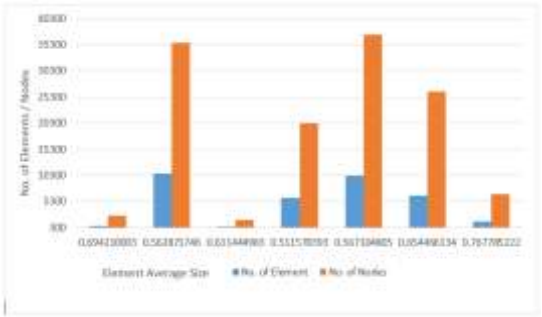

Figure 41 Element Size versus No of Element and Nodes

Various types of interfaces are available in ANSYS -16.2 software, Defining contacts between the imported geometry assembled parts. This approach gives results that are more accurate but is time-consuming. Bonded contact is very common type of contact, which frequently used in FEA in Ansys Bonded contact allows all the nodes of an unstructured Part in the model to be bonded to a face of another unstructured Part. Apart from this, we have contact options as no separation, Frictional etc. however we completed analysis using another way to define the connection is joints. This is was most suitable and only way to provide connection since we carried out the static and transient analysis of Robotic gripper. In this, we have two types of joint one is Body to Ground and Body to Body. Joints detail shown below in figures.

c. Static Finite Element Analysis

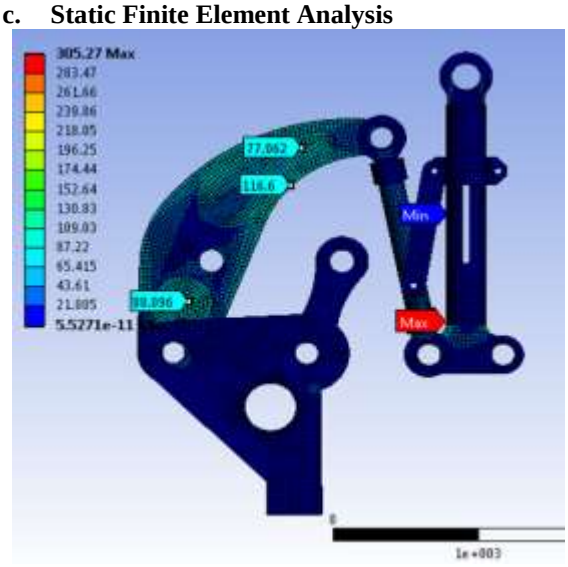

Figure 42 Von Mises Stress Plot

The results of Maximum Von-Mises stress with maximum value of 305.27 MPa and Deformation with Maximum value of 3.65 mm. Also shows energy transformation and the critical areas that need be reiteration in future to improve the results.

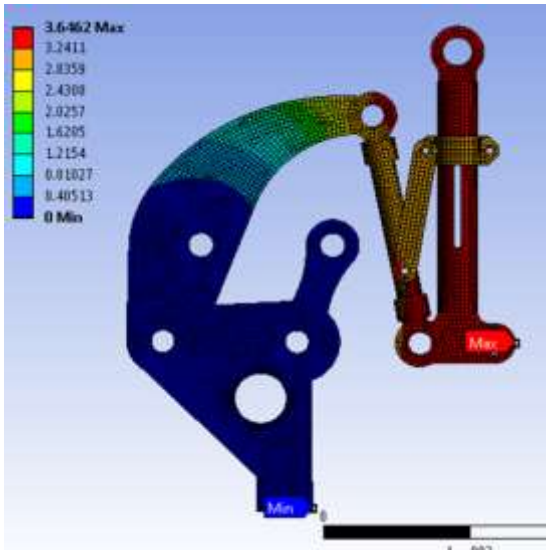

Figure 43 Deformation Plot

d. Transient Structural Finite Element Analysis

In transient analysis, the loads fluctuate with time instance. Normally in Mechanical systems, we can use a transient analysis on flexible assemblies moreover a rigid structures. For Robotic gripper application, we have used the solver as ANSYS - Mechanical - APDL to solve a Transient Structural analysis however, there are other solvers such as Samcef, or ABAQUS also used extensively.

In here, we used to find the dynamic response of an assembly under the action of loads, which is fluctuating with time. We have also found the changes in deformations and stresses with respect to time instances.

A transient structural analysis is extra intricate than a static analysis since it generally requires further processer resources, for solving the problem. We can reduce this time by taking primary effort to recognize the behavior of the problem.

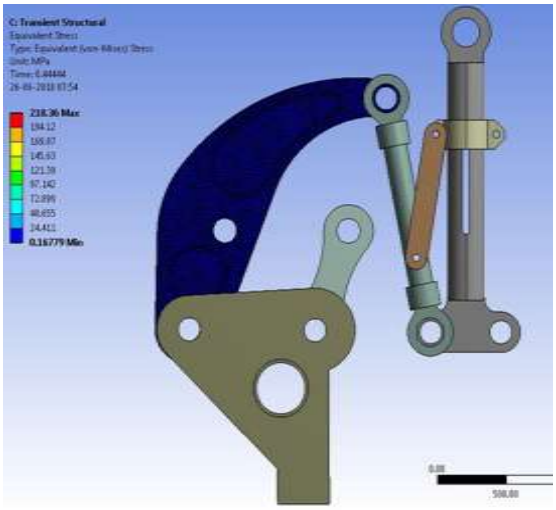

Figure 44 Transient Analysis – Eq. Stress –Position 2

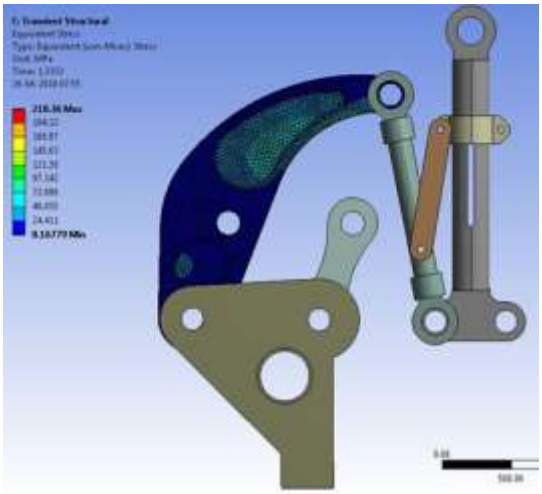

Figure 45 Transient Analysis – Eq. Stress –Position 2

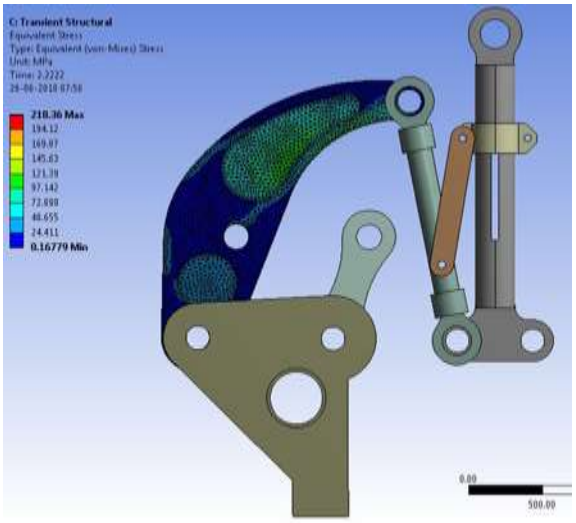

Figure 46 Transient Analysis – Eq. Stress –Position 3

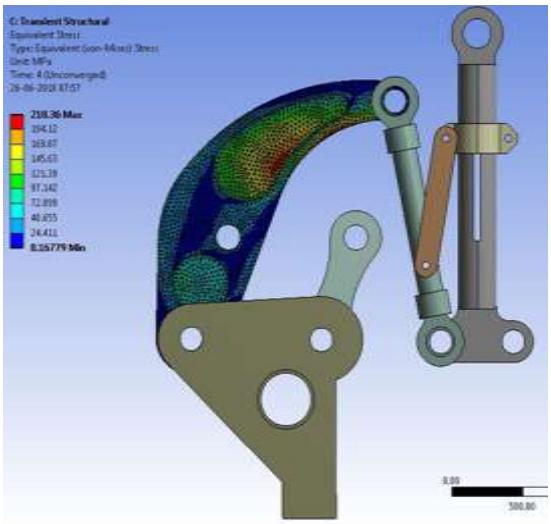

Figure 47 Transient Analysis – Eq. Stress –Position 4

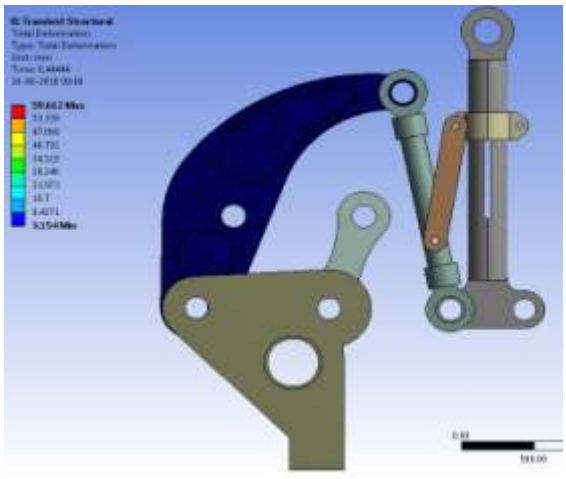

Figure 48 Transient Analysis – Deformation – Position 1

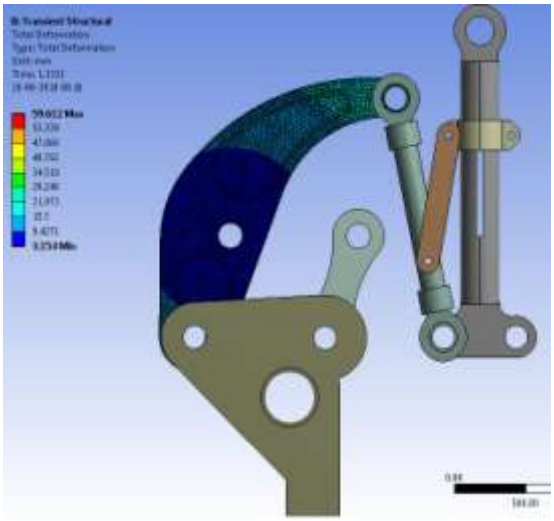

Figure 49 Transient Analysis – Deformation– Position 2

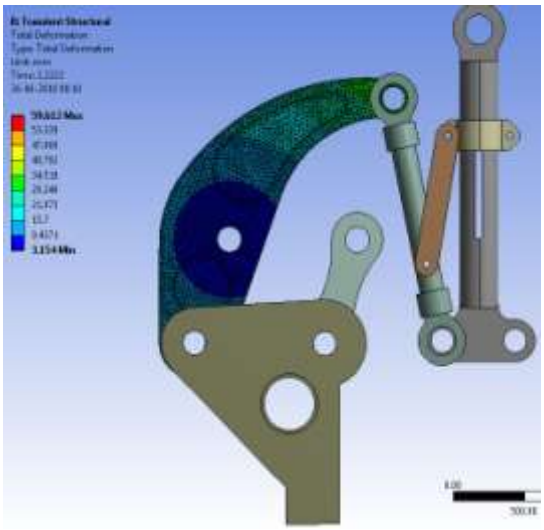

Figure 50 Transient Analysis – Deformation– Position 3

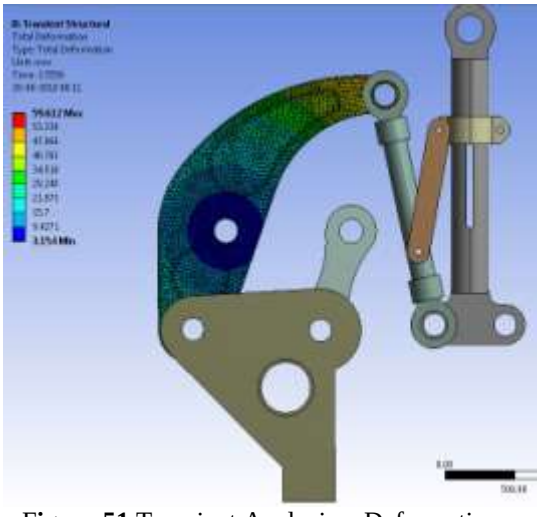

Figure 51 Transient Analysis – Deformation– Position 4

VIII. CONCLUSION

This thesis categorized in three phases of analysis of Impactive Robotic Grippers. (i) Kinematic synthesis (ii) Static Analysis (iii) Dynamic Analysis and (iv) FEA

In kinematic synthesis, the mechanism studied for different types of motion as well as the different speed ratings and its effects on linkages has studied on software MSC Adam 2013. Graphical method used for the validation of this computational kinematics synthesis. The results of this validation shows the close relevance with calculated values of displacements, velocity and acceleration from simulated values from MSC Adams.

The robotic gripper is simulated for 225 KN Load. The MSC Adams results generated from simulation of Robotic gripper shows that the effort required to hold the object is inversely proportional to angle 'α' and directly proportional to distance between Jaws. Validation of static analysis carried out by the analytical manual computation to determine the efforts required to hold the object firmly and both the results appears in precise significance each other.

During later phase of analysis of dynamic effects along with software packages such as MSC Adams and ANSYS Workbench 16.2 is used. To get the desired motion displacement of driven component that is gripper jaws the driving component was applied with force of F = 259.5 KN. Itis observe that the mechanism requires the force, which is about 150 KN to start the motion by overcoming the mass inertia of the several component however; the entire mechanism keeps on oscillating because of unbalanced inertias. Then to understand effect of sinusoidal force of magnitude of 1.4F applied to the driving component. Under this condition, the mechanism oscillates and velocity and accelerations fluctuates a lot. This is because of sinusoidal nature of force caused by simple harmonic motion. Similarly, the analysis with Sinusoidal Force Magnitude is double 2 x 1.4 x F carried out to check the system response. We can conclude that the oscillations increase with increase in magnitude of sinusoidal force.

In the final FEA phase, static study results of von Mises stresses and deformation with maximum values of 305.27 MPa and of 3.65 mm. In this transient analysis, our area of interest was Part 5 Main Arm. The transient analysis shows the variation in stresses and deformation at different instances.

After carrying out the present work, still work may extend to develop vibration analysis and Optimization of Robotic Gripper.

REFERENCES

[1]. Bai, G. (2016). Kinematic analysis and dimensional synthesis of a meso-gripper. ASME 2016 International Design Engineering Technical Conferences 2016.
[2]. Birglen, L. (2017). A statistical review of industrial robotic grippers. ELSEVIER Robotics and Computer–Integrated Manufacturing.
[3]. Campeau-Lecours, A. (2017). An articulated assistive robot for intuitive hands-on-payload manipulation. ELSEVIER Robotics and Computer–Integrated Manufacturing.
[4]. Causey, G. (2003). Guidelines for the design of robotic gripping systems . MCB UP Ltd / Emerald Group Publishing.
[5]. Chappell, P. (1999). Kinematic control of a three-fingered and fully adaptive end-effector using a Jacobian matrix. ELSEVIER Mechatronics.
[6]. Dalibor Petkovi, e. a. (2016). Analyzing of flexible gripper by computational intelligence approach. ELSEVIER Mechatronics.
[7]. FantonI, G. (2014). Method for supporting the selection of robot grippers. ELSEVIER Procedia CIRP.
[8]. Giulio Rosati, e. a. (2017). Design & const. of a variable aperture gripper for flexible automated assembly.
[9]. Han, L. (2016). Design Simulation of a Handling Robot for Bagged Agricultural Materials. ELSEVIER IFAC-Papers Online.
[10]. Hassana, A. (2016). Modeling and design optimization of a robot gripper mechanism. ELSEVIER Robotics and Computer–Integrated Manufacturing(2001).
[11]. International Federation of Robotics (IFR). (2016). Executive Summary World Robotics 2016 Industrial Robots. Retrieved from https://ifr.org/: https://ifr.org/img/uploads/Executive_Summary_WR_Industrial_Robots_20161.pdf
[12]. Kurfess, T. R. (2005). ROBOTICS AND AUTOMATION HANDBOOK. Boca Raton London New York Washington D.C.: CRC PRESS.
[13]. Lee., J. (2003). Kinematic synthesis of Industrial Robot Gripper A Creative Design Approach. ELSEVIER Robotics and Autonomous Systems (2003).
[14]. Melchiorri., C. (1997). Multiple whole-limb manipulation: An analysis in the force domain. ELSEVIER Robotics and Autonomous Systems.
[15]. Moghaddam, M. (2016). Parallelism of Pick-and-Place operations by multi-gripper robotic arms. ELSEVIER Robotics and Computer–Integrated Manufacturing.
[16]. Nguyen, C. C. (2003). Dynamic analysis of a 6 dof CKCM robot end-effector for dual-arm tele robot systems. ELSEVIER Robotics and Autonomous Systems.
[17]. Rituparna Datta, S. P. (2015). Analysis and Design Optimization of a Robotic Gripper Using Multi-objective Genetic Algorithm. Analysis and Design Optimization of a Robotic Gripper Using Multi-objective Genetic Algorithm.
[18]. Robotics Breakthroughs From the Past Decade. (n.d.). Retrieved from Mashable: http://mashable.com/2013/10/23/robotics-breakthroughs/#IbGvIv9uiaqX
[19]. RobotShop Distribution Inc. (2008). http://www.robotshop.com/media/files/PDF/timeline. Retrieved from www.robotshop.com: http://www.robotshop.com/media/files/PDF/timeline.pdf

Sachin Badadhe "Computer Aided Kinematic Synthesis Anddynamic Analysis Of Robot End Gripper Mechanism "'International Journal of Engineering Research and Applications (IJERA) , vol. 8, no.10, 2018, pp 30-45